

Numerical Simulation of Local Scour with Free Surface and Automatic Mesh Deformation

Xiaofeng Liu¹ and Marcelo H. García²

¹Research Assistant, Ven Te Chow Hydrosystems Laboratory, Department of Civil and Environmental Engineering, University of Illinois at Urbana and Champaign, 205 N Mathews Ave., Urbana, IL 61801. E-mail: liu19@uiuc.edu.

²Chester and Helen Siess Professor, and Director, Ven Te Chow Hydrosystems Laboratory, Department of Civil and Environmental Engineering, University of Illinois at Urbana and Champaign, 205 N Mathews Ave., Urbana, IL 61801. E-mail: mhgarci@uiuc.edu.

ABSTRACT

A numerical model for local scour with free surface and automatic mesh deformation is constructed and numerical simulation is carried out to compare with experimental results. The $k-\epsilon$ model is used to simulate the turbulent flow field. Two interfaces (water and air, water and sediment) in the domain are captured with different approaches. The free surface of the flow is captured by Volume of Fluid (VOF) scheme which is a Eulerian approach. The water-sediment interface (bed) is captured with moving mesh method which is a Lagrangian approach. The flow field is coupled with sediment transport using a quasi-steady approach. Good results have been obtained using current model. The flow field is comparable with the experiment. Scour patterns are similar to the experimental data.

INTRODUCTION

In this paper, a new numerical model is proposed to simulate the scour process together with free surface and automatic mesh deformation. In scour problem, there are two sharp interfaces: water-air and water-sediment. The two interfaces are captured using different methods. The water-air interface is captured by Eulerian method, namely VOF method. The water-bottom interface is captured by Lagrangian method, namely moving mesh method.

In numerical simulation of open channel flow, free water surface is usually replaced by a rigid lid. This is valid only if the free surface does not change too much along the channel. There are many surface tracking or capturing method available to simulate the free surface, e.g. marker and cell (MAC) method, volume of fluid method (VOF) method (Hirt and Nicholls 1981), level set method (Sethian 1996). In this paper, a high resolution VOF method proposed by Ubbink and Issa (1999) is chosen to track the free surface. The CICSAM (Compressive Interface Capturing Scheme for Arbitrary Meshes) scheme treat the whole domain as the mixture of two liquids. Volume fraction of each liquid is used as the weighting factor to get the mixture properties, such as density, viscosity.

In scour problem, the bed deformation is coupled with the transient flow field. Brørs (1999) used structured grid to model the scour under pipelines. The grid on the bed and the corresponding grids above were moved according to the bed elevation change. This method for structured grids is similar to manually moving each grid point at each time step and is not efficient. In unstructured grids, it is more complicated to move the grid points on the bed and in the domain. Arbitrary movement of the points may invalidate the grid. In this paper, an automatic grid movement algorithm is used to avoid these problems. There are many mesh deformation method developed in the past years, such as spring analogy, Laplacian operator smoothing. The latter is chosen in this paper because it is more robust and easy to implement in unstructured grid for complex domain. The Laplacian operator method is to solve the Laplacian equation with the deformation condition on the boundary. This will smoothly deform the inner grid.

GOVERNING EQUATIONS

Fluid Part—Navier-Stokes Equations

The governing equations for the fluid part is the Navier-Stokes equations:

$$\nabla \cdot \mathbf{u} = 0 \quad (1)$$

$$\frac{\partial \rho \mathbf{u}}{\partial t} + \nabla \cdot (\rho \mathbf{u} \mathbf{u}) - \nabla \cdot (\mu \mathbf{S}) = -\nabla p + \rho \mathbf{g} + \sigma K \frac{\nabla \alpha}{|\nabla \alpha|} \quad (2)$$

where \mathbf{u} is the velocity vector field, p is the pressure field, α is the volume fraction function for the two fluids defined by

$$\alpha = \begin{cases} 0 & \text{volume occupied by air} \\ 1 & \text{volume occupied by water} \end{cases} \quad (3)$$

\mathbf{S} is the strain rate tensor defined by $\mathbf{S} = \frac{1}{2}(\nabla \mathbf{u} + \nabla \mathbf{u}^T)$. σ is surface tension, K is the surface curvature. Surface tension is not so important in scour problem but it's included for completeness. The density ρ and viscosity μ in the domain is given by

$$\rho = \alpha \rho_1 + (1 - \alpha) \rho_2 \quad (4)$$

$$\mu = \alpha \mu_1 + (1 - \alpha) \mu_2 \quad (5)$$

Volume fraction α is transported by the fluid velocity field. The equation for the volume fraction scalar α is

$$\frac{\partial \alpha}{\partial t} + \nabla \cdot (\mathbf{u} \alpha) = 0 \quad (6)$$

Numerical diffusion will spread out the sharp interface between water and air. An compressive interface capturing scheme CICSAM is used to resharpen the interface. The details of the present free surface modeling and CICSAM scheme can be found in Ubbink and Issa (1999).

Equations in fluid part are closed by conventional k - ϵ model (Lauder and Spalding 1973).

$$\mu_t = C_\mu \rho \frac{k^2}{\epsilon} \quad (7)$$

$$\frac{\partial k}{\partial t} + \nabla \cdot (\mathbf{u}k) = \frac{1}{\rho} \nabla \cdot \left(\frac{\mu_t}{\sigma_k} \nabla k \right) + 2 \frac{\mu_t}{\rho} |\nabla \mathbf{u}|^2 - \epsilon \quad (8)$$

$$\frac{\partial \epsilon}{\partial t} + \nabla \cdot (\mathbf{u}\epsilon) = \frac{1}{\rho} \nabla \cdot \left(\frac{\mu_t}{\sigma_\epsilon} \nabla \epsilon \right) + 2 \frac{C_1 \mu_t}{\rho} |\nabla \mathbf{u}|^2 \frac{\epsilon}{k} - C_2 \frac{\epsilon^2}{k} \quad (9)$$

where μ_t is turbulence eddy viscosity, k is turbulence kinetic energy and ϵ is turbulence energy dissipation rate. The constants appear in Eqs. (7), (8) and (9) take the values given in Lauder and Spalding (1973).

Sediment Transport Part

Scour problem is caused by the movement of sediment. In this numerical model, only bed load is considered. Exner equation is used to updated the bed elevation. There are many bed load transport rate formulas in the literature. Most of them relate bed load transport rate with shear stress. The formula in Engelund and Fredsøe (1976) is chosen in this model

$$q^* = \begin{cases} 18.74(\theta - \theta_c) \left[\theta^{1/2} - 0.7\theta_c^{1/2} \right] & \text{if } \theta > \theta_c \\ 0 & \text{otherwise} \end{cases} \quad (10)$$

where q^* is a dimensionless bed load transport rate known as Einstein number given by

$$q^* = \frac{q_0}{\sqrt{Rgdd}}$$

here q_0 is the bed load transport rate for flat bed. θ and θ_c are Shields number and critical Shields number respectively, where θ is defined as:

$$\theta = \frac{\tau_b}{\rho g R d}$$

where τ_b is the bed shear stress calculated from the fluid part, ρ is the density of water, g is the gravitational acceleration, R is the specific gravity of sediment, d is the sediment grain diameter.

The critical Shields number for a particular sediment is always given for flat bed and it should be adjusted according to the local slope of the bed and local shear force direction. The critical Shields number for flat bed, θ_{c0} , is always given as a constant. The approach used here to account the slope effect is similar to that in Brørs (1999) but with an extension to three dimensions. Figure 1 is the scheme of the adjustment where \vec{n} is the surface normal, \vec{S} is the steepest slope and $\vec{\tau}$ is the wall shear stress vector acting on the bed. The critical Shields number is adjusted according to

$$\theta_c = \theta_{c0} \frac{\sin(\alpha - \text{sgn}(\vec{\tau} \cdot \vec{S})\phi)}{\sin(\alpha)} \quad (11)$$

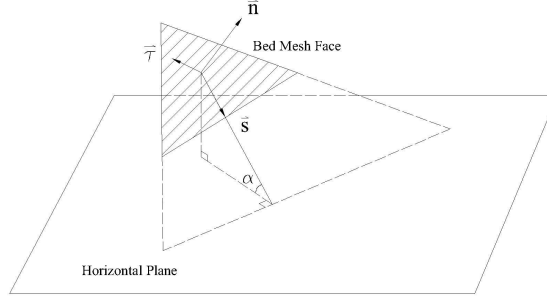


Figure 1. Slope Effect on Sediment Transport

where α is the slope angle of the bed, ϕ is the internal friction angle of sediment. sgn is the sign function which returns the sign of the variable. Eq. 10 only gives the total bed load. The bed load transport rates in different directions are given by

$$q_i = q_0 \frac{\tau_i}{|\tau|} - C |q_0| \frac{\partial h}{\partial x_i}, i = 1, 2 \quad (12)$$

where C is a constant in the range of 1.5-2.3 which is used to reflect the slope effect on the sediment flux (Brørs 1999).

Bed Change Model—Exner Equation

The bed elevation change is based on the continuity of sediment. The Exner equation, which describes the sediment continuity, is

$$\frac{\partial h}{\partial t} = \frac{1}{1-n} [-\nabla \cdot \mathbf{q}] \quad (13)$$

where h is the bed elevation, n is the porosity of the bed, \mathbf{q} is the bed load transport rate vector whose components are given by Eq. 12.

Mesh Deformation Solver—Laplacian Equation

Governing equations for the mesh motion equation is Laplacian equation (Jasak and Tukovic 2005). Let \mathbf{v} be the grid motion velocity field, then the equation becomes

$$\nabla \cdot (\gamma \nabla \mathbf{v}) = 0 \quad (14)$$

where γ is the diffusion coefficient chosen to control the mesh motion. γ can be a constant or a variable defined by other properties in the domain. The choice of variable γ depends on the specific mesh motion problem and needs objective judgement. Jasak and Tukovic (2005) suggested several possibilities to set the γ value based on distance from some boundary or mesh qualities. In this research, γ is set as a non-zero constant for simplicity. The boundary condition for Eq. 14 is given by Exner equation. When

the grid motion velocity field is solved, the grids in the whole domain can be moved based on the equation

$$\mathbf{x}^{k+1} = \mathbf{x}^k + \mathbf{v}\Delta t \quad (15)$$

Here, \mathbf{x}^{k+1} and \mathbf{x}^k are grid position vectors at time level $k + 1$ and k respectively, and Δt is the time step.

NUMERICAL SIMULATION SCHEMES AND PROCEDURE

The governing equations in the previous section form a big coupled system. The code used in this research is the open source CFD code OpenFOAM (2005). It's freely available through internet. OpenFOAM is primarily designed for problems in continuum mechanics. It uses the tensorial approach and object oriented techniques (Weller et al. 1998). OpenFOAM provides a fundamental platform to write new solvers for different problems as long as the problem can be written in tensorial partial differential equation forms. In this research, the flow field is solved by the adaption of the original turbulence solver for incompressible fluid. The sediment transport equation and bed deformation is added to this to form a new solver called FOAMSCOUR. The finite volume details of the code can be found in Jasak (1996).

Numerical Scheme for Flow Field

For pressure-velocity coupling in Navier-Stokes equation, many schemes exist, such as SIMPLE (Patankar 1981) and PISO (Issa 1986). PISO scheme is used in this code. For the $k - \epsilon$ turbulence model equations, although k and ϵ equations are coupled together, they are solved by segregated approach.

Numerical Scheme for Sediment Part

The bedload load in sediment transport are solved very easily since when the shear stress on the bottom is obtained from the flow solver, using Eq. 10 to calculate the bedload is straightforward. After the sediment load is calculated, the Exner equation is solved to change the bed elevation. Careful examination of the Exner equation will find that it's a 2D equation. The bed elevation change is due to the divergence of sediment transport flux. This simple 2D equation can usually be solved by finite difference method using structured grid when the bottom has a regular shape (Brørs 1999; Olsen and Melaaen 1999). For complex domains, finite volume or finite element method can be used with unstructured grids. In this research, two meshes are used. One is for the fluid solver and the other is for the bottom Exner equation. The Exner equation is solved on the 2D bottom mesh using finite volume method. In Figure 2, it's shown that the coupled problem is solved through mapping between the fluid mesh bottom boundary and sediment 2D mesh. After the flow solver and turbulence solver is finished, the shear stress is mapped from 3D fluid bottom boundary to 2D sediment mesh. On the 2D sediment mesh, the Exner equation is solved and the new bed elevation is calculated. Then the bed elevation is mapped back from 2D sediment mesh to 3D fluid mesh. The 3D fluid mesh is deformed according to this as a boundary condition.

Numerical Scheme for Automatic Mesh Deformation

A finite volume solver for the Laplacian equation is written and it's used on the 3D fluid mesh to move the grid points. The mesh movement quantities are solved for the

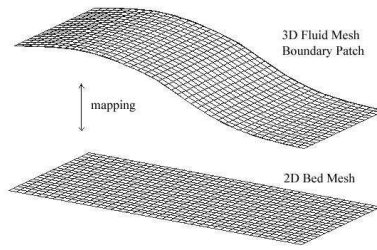


Figure 2. Bed Grid Mapping(From 3D to 2D)

cell centers. After those center values are obtained, they are interpolated to the grid points to do the actual mesh motion.

Simulation Flow Chart

The flow chart of the simulation is plotted in Figure 3. A quasi-steady approach is used in the model. When the flow field is being calculated, the domain boundaries are fixed. Only at the sediment movement step, the domain boundaries are adjusted. In order to increase the accuracy, smaller time steps are used at the beginning of the simulation when the bed movement is fast. After the flow field and bed change reach relatively steady state, bigger time steps can be used to accelerate the computation.

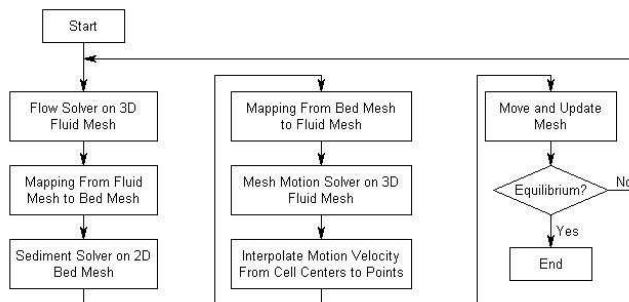


Figure 3. Flow chart of the computation

MODEL APPLICATION

In this section, applications of wave scour around big pile (3D case) are carried out using FOAMSCOUR and compared with experimental data. In wave scour around big pile, the water wave and its interaction with pile are important. Coupled problem of flow field with morphodynamics usually takes a very long time for computation. Parallel computing with domain decomposition is used to accelerate the process. All computations are done on NCSA Tungsten Xeon Cluster in University of Illinois at Urbana and Champaign.

Scour process around vertical pile caused by wave is more complicated because of the 3D nature of the problem. The test case uses the experimental data by Sumer and Fredsoe (2001). The schematic view of the experiment is shown in Figure 4. Test case 7 of the experiment is used in this paper. In this case, the wave has a period

of 3.5s, wave height of 6.4cm, wave length of 6.79m and Keulegan-Carpenter (KC) number of 0.61. The pile has a diameter of 1m and the sand has $d_{50} = 0.2mm$ and Shields parameter of 0.07. The wave in the experiment is generated by a piston type

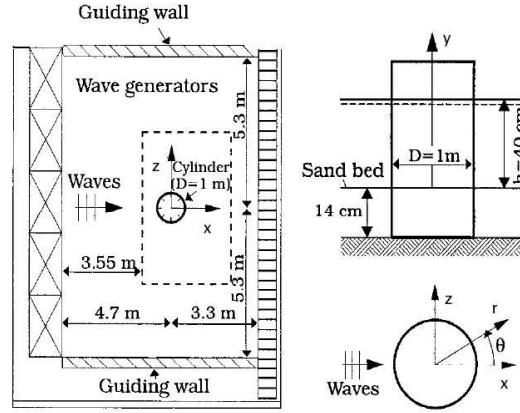


Figure 4. Wave Scour Around Big Pile Scheme (After Sumer and Fredsøe (2001))

wave maker and at the end of the wave tank, there is a wave absorber to eliminate the wave reflection. In numerical simulation, the wave can be generated generally by two approach: moving mesh (Aliabadi et al. 2003) and wave boundary condition (Mayer et al. 1998). For moving mesh approach, the piston movement is simulated by moving the boundary of the computational domain. For wave boundary condition approach, the mesh is fixed but boundary condition on the piston part is given by wave theory. The second approach is adopted in this paper. A time varying velocity profile is imposed at the piston boundary to generate the waves

$$\vec{U} = f_r(t) \left[\vec{U}(y) \sin(\omega t + \theta) \right] \quad (16)$$

where \vec{U} is the velocity vector at the boundary, ω is the wave frequency, θ is the phase. $\vec{U}(y)$ is imposed by the type of the piston. $f_r(t)$ is the "ramp" function to start up the piston. $f_r(t)$ has the form

$$f_r(t) = \begin{cases} \frac{t}{T} - \frac{1}{\pi} \sin\left(\pi \frac{t}{T}\right) & \text{for } 0 < t < T \\ 1 & \text{for } t > T \end{cases} \quad (17)$$

where T is the wave period.

The wave absorber is simulated using a damping zone (or sponge layer). In this damping zone, extra fluid viscosity is added to the momentum equation to dissipate the fluid dynamic energy. An alternative method by modifying the water depth and fluid velocity in the damping zone can be found in Mayer et al. (1998).

Figure 5 shows an instantaneous free surface of the wave. A probe point ($x=5.7m$ $y=0.2m$ $z=5.3m$) is also indicated in the figure. Figure 6 shows the pressure change

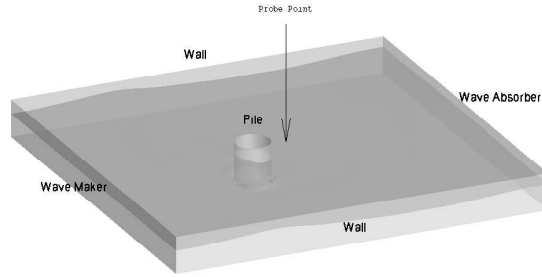


Figure 5. Free Surface of The Wave

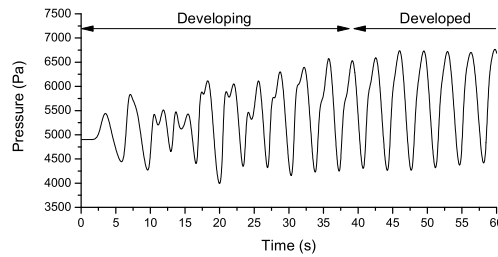


Figure 6. Pressure Probe at Point ($x=5.7\text{m}$ $y=0.2\text{m}$ $z=5.3\text{m}$)

with time at the probe point. At the first several period of time, the wave is under development and the pressure has some noise. But when the wave is fully developed, the pressure is undergoing sinusoidal cycles as desired. Figure 7 shows the equilibrium state of the scour around the pile. The numerical result is comparable with the experimental data although the maximum scour depth of numerical simulation is a little higher than the experiment result. As in the experiment, the deposition zone is on the side of the pile and the scour zone is in the front and back. Although the scour pattern is not identical to that of experiment result, they are very similar. Figure 7(d) shows the scour around the periphery of of the cylinder base. Only half of the periphery is shown because of symmetry. From this figure, the scour and deposition pattern around the pile agrees well with the experiment except the amplitude and some details. This may be caused by the fact that some other factors in the experiment are not included in the numerical model. Further research is needed to make the model more accurate.

DISCUSSION

In rigid lid approach, the free surface is replaced with an imaginary horizontal frictionless plane. But in wave scour problem, it's unreasonable to use the rigid lid approximation. Free surface capturing or tracking should be used to simulate the wave scour process.

The two moving surfaces(water free surface and moving bed) in current model Eulerian and Lagrangian approaches. The scour test case in the paper is relatively simple. For more complicated problems, if the interface between the object, water and bed is irregular, simply moving the grid point along the interface will be highly non-applicable. Also when the amplitude of the boundary movement is big enough, the mesh may be

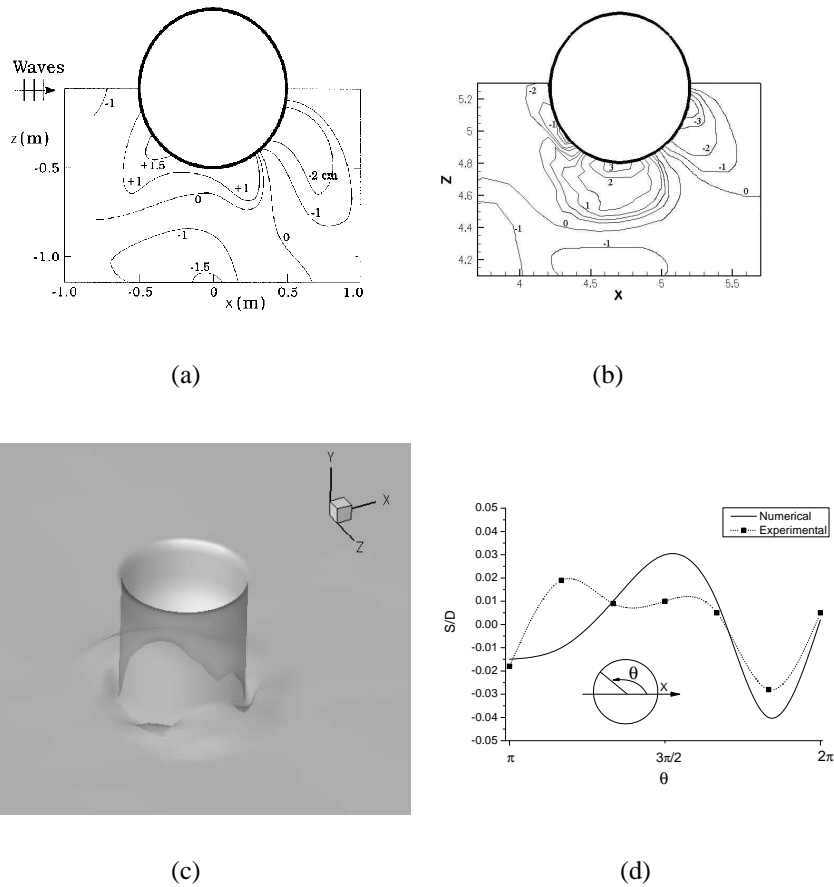


Figure 7. Wave Scour Around Big Pile: (a) Experimental Data (b) Numerical Result (c) 3D View of Numerical Result (d) Scour at Periphery of Cylinder Base

highly distorted and the deteriorated mesh quality will make the computation not easy to converge. Mesh cells should be split or merged when necessary. This is called dynamic mesh method. But comparing with mesh deformation, it is more difficult to be implemented. Combination of these two approaches can be promising.

CONCLUSIONS

Numerical model FOAMSCOUR for local scour with free surface and automatic mesh deformation is constructed. Good results have been obtained using current model. Velocity field and other flow field characteristics are comparable with experiment. The maximum scour depths and local scour profile fit well with the experiment data. Further research is needed to make current numerical model more accurate. The free surface is modeled by VOF method while the scour process is modeled by moving mesh method. These two methods for moving boundaries (free surface and bed) are coupled together. Eulerian approach can be used to capture the complex scour profiles.

ACKNOWLEDGMENTS

The support from the coastal Geoscience Program of the U.S. Office of Naval Research (Grant N00014-05-1-0083) is gratefully acknowledged.

REFERENCES

- Aliabadi, S., Abedi, J., Zellars, B., Bota, K., and Johnson, A. (2003). "Simulation technique for wave generation." *Communications in Numerical Methods in Engineering*, (19), 349–359.
- Brørs, B. (1999). "Numerical modeling of flow and scour at pipelines." *Journal of Hydraulic Engineering*, 125(5), 511–523.
- Engelund, F. and Fredsøe, J. (1976). "A sediment transport model for straight alluvial channels." *Nordic Hydrology*, 7, 293–306.
- Hirt, C. and Nicholls, B. (1981). "Volume of fluid (vof) method for dynamics of free boundaries." *Journal of Computational Physics*, 39(1), 201–225.
- Issa, R. (1986). "Solution of the implicitly discretised fluid flow equations by operator-splitting." *Journal of Computational Physics*, 62(1), 40–65.
- Jasak, H. (1996). "Error analysis and estimation for the finite volume method with application to fluid flows," PhD thesis, Imperial College of Science, Technology and Medicine.
- Jasak, H. and Tukovic, Z. (2005). "Automatic mesh motion for the unstructured finite volume method.." *submitted to Journal of Computational Physics*.
- Lauder, B. and Spalding, D. (1973). "The numerical computation of turbulent flows." *Computer Methods in Applied Mechanics and Engineering*, 3(2), 269–289.
- Mayer, S., Garapon, A., and Sorensen, L. (1998). "A fractional step method for unsteady free-surface flow with application to non-linear wave dynamics." *International Journal For Numerical Methods in Fluids*, (28), 293–315.
- Olsen, N. R. and Melaaen, M. (1999). "Three-dimensional numerical flow modeling for estimation of maximum local scour depth." *Journal of Hydraulic Research*, 36(9), 579–590.
- OpenFOAM (2005). <http://www.OpenFoam.org>.
- Patankar, S. (1981). *Numerical Heat Transfer and Fluid Flow*. McGraw-Hill.
- Sethian, J. (1996). *Level Set Methods: Evolving Interfaces in Geometry, Fluid Mechanics, Computer Vision, and Material Science*. Cambridge Monographs on Applied and Computational Mathematics. Cambridge University Press.
- Sumer, B. and Fredsoe, J. (2001). "Wave scour around a large verticle circular cylinder." *Journal of Waterway, Port, Coastal and Ocean Engineering*, 127(3), 125–134.
- Ubbink, O. and Issa, R. (1999). "A method for capturing sharp fluid interfaces on arbitrary meshes." *Journal of Computatonal Physics*, 153, 26–50.
- Weller, H., Tabor, G., Jasak, H., and Fureby, C. (1998). "A tensorial approach to computational continuum mechanics using object-oriented techniques." *Computers in Physics*, 12(6), 620–631.